# Avoiding numerical pitfalls in social force models

Gerta Köster,* Franz Treml, and Marion Gödel
*Department of Computer Science and Mathematics, Munich University of Applied Sciences, 80335 Munich, Germany*
(Received 16 January 2013; published 14 June 2013)

The social force model of Helbing and Molnár is one of the best known approaches to simulate pedestrian motion, a collective phenomenon with nonlinear dynamics. It is based on the idea that the Newtonian laws of motion mostly carry over to pedestrian motion so that human trajectories can be computed by solving a set of ordinary differential equations for velocity and acceleration. The beauty and simplicity of this ansatz are strong reasons for its wide spread. However, the numerical implementation is not without pitfalls. Oscillations, collisions, and instabilities occur even for very small step sizes. Classic solution ideas from molecular dynamics do not apply to the problem because the system is not Hamiltonian despite its source of inspiration. Looking at the model through the eyes of a mathematician, however, we realize that the right hand side of the differential equation is nondifferentiable and even discontinuous at critical locations. This produces undesirable behavior in the exact solution and, at best, severe loss of accuracy in efficient numerical schemes even in short range simulations. We suggest a very simple mollified version of the social force model that conserves the desired dynamic properties of the original many-body system but elegantly and cost efficiently resolves several of the issues concerning stability and numerical resolution.

DOI: 10.1103/PhysRevE.87.063305 PACS number(s): 02.60.−x, 89.40.−a, 95.75.Pq, 45.70.Vn

## I. INTRODUCTION

There are many approaches to modeling pedestrian dynamics [1–4]. Among them social force models are well established [5,6]. Their proximity to equations derived from Newton's laws of motion allow direct application of standard numerical methods, such as Euler's method, to solve the equations that are available through toolboxes such as Matlab, Mathematica, or numerical libraries. Nonetheless, scientists and tool users continue to run into trouble when implementing or employing the model [7,8].

While the physical properties of the model that do not match human behavior, such as inertia, have been discussed to some extent [8], very little attention has yet been paid to the mathematical properties and the resulting effects on the stability of the supposed exact solution and numerical solution attempts. In fact, the authors are not aware of a general proof of existence for the solution. Discussions of stability refer to strongly simplified one-dimensional problems [9].

The social force model resembles a Newtonian system without being Hamiltonian itself. Energy conservation is destroyed by friction and an upper limit for pedestrian speed. See [10,11] for extensive discussions of Hamiltonian systems. Hence, classic methods from molecular dynamics that make use of the Hamiltonian form do not target the problem and we need to look for other solution options.

In this work, we point out several mathematical properties of the right hand side of the social force model's set of differential equations that lead to oscillations in the solution and loss of accuracy in the numerical approximation. As a matter of fact, the discrete difference equations that the numerical schemes correspond to have solutions that do not only quantitatively differ from the supposed solution of the social force model, but also qualitatively. This background analysis is described in Sec. II. In Sec. III, we suggest ways to mollify the right hand side so that the difficulties disappear, while the desired properties of the original model are conserved. In Sec. IV, we demonstrate the success of our ideas by comparing numerical solutions of both models at strategically important locations in very simple simulation scenarios that allow isolating the underlying problems.

Finally, in Sec. V, we compare results for the classic and the mollified model in a typical bottleneck scenario taken from [12]. We use numerical schemes with step sizes that produce errors of comparable size as long as no singularity is encountered. Not only do the results for the mollified model prove to be more natural but, in addition, we are able to utilize a much more efficient fifth order Runge-Kutta scheme saving considerable simulation time.

## II. PROBLEM ANALYSIS

### A. Original social force model of Helbing and Molnár

This work is built upon the original equations as they were presented in [5] and in Molnár's dissertation [13]. We are aware that most simulation tools based on the social force model (SFM) use variations of the base model. But, these variations still have the essential properties of the original and hence will experience similar difficulties.

We look at vectors $x, v \in \mathbb{R}^{2\times m}$ that denote the location and velocity of pedestrians $1,\ldots,m$ in two-dimensional Euclidean space. Vertical movement is neglected. To make sure that the speed of an individual $j$ does not exceed an acceptable upper limit $v_{\max,j}$, we need the auxiliary velocity $w$ in the mathematical formulation. Note that imposing a limit on pedestrian speed introduces a first deviation from Newtonian mechanics. When the speed is cut off without compensation, energy is lost. Following [5], we set $v_{\max,j} = 1.3\, v_{0,j}$ where $v_{0,j}$ is each pedestrian's individual free-flow velocity. Hence, pedestrians can accelerate but will not sprint. For the $j$th pedestrian, we have

$$\dot{x}_j = v_j(w_j) := \begin{cases} w_j & \text{if} \quad \|w_j\| < v_{\max,j} \\ \frac{v_{0,j}}{\|w_j\|} w_j & \text{otherwise.} \end{cases} \tag{1}$$

*gerta.koester@hm.edu

 

The following set of equations for $x$ and $w$ forms the actual social force model:

$$\begin{aligned} \dot{x} &= v(w), \\ \dot{w} &= F(x,w) = F_{\text{target}}(x,w) + F_{\text{ped}}(x,w) + F_{\text{ob}}(x,w). \end{aligned} \tag{2}$$

$F_{\text{target}}$, $F_{\text{ped}}$, and $F_{\text{ob}}$ stand for forces acting on each pedestrian from the attracting target(s), repelling fellow pedestrians, and repelling obstacles. Forces are assumed to obey a superposition principle. Since there are usually several interacting pedestrians and several obstacles, $F_{\text{ped}}$ and $F_{\text{ob}}$ are sums of force terms $F_{\text{ped},i,j}$ and $F_{\text{ob},k}$. $F_{\text{ped}}$ and $F_{\text{ob}}$ are expressed as the gradients (in $x$) of suitable potentials, but not $F_{\text{target}}$ as we will discuss in Sec. II B.

Most of our observations are best presented when the system is reduced to the bare essentials. Hence, we will assume one target, one or two pedestrians depending on the scenario, and no obstacle, all unless otherwise stated. The resulting mathematical claims can easily be carried over to more complex situations.

### B. Behavior at the target: Discontinuity of the right hand side

In this section, we will look at the seemingly trivial situation of one pedestrian moving towards one target in a space free of obstacles. We may drop the index for the pedestrian and force types. We also neglect, for the moment, that the velocity is bounded but will come back to the implications of the cutoff function in Sec. II D. We consider the simplified equations

$$\begin{aligned} (\dot{x}_1,\dot{x}_2) &= (v_1,v_2), \\ (\dot{v}_1,\dot{v}_2) &= F((x_1,x_2),(v_1,v_2)). \end{aligned} \tag{3}$$

Without loss of generality, we set the target location to (0,0). Force $F$ then has the form

$$F(x,v) = \frac{1}{\tau}\left(-\frac{x}{\|x\|}v_0 - v\right). \tag{4}$$

The free-flow velocity $v_0$ is the presumed walking velocity of an individual across an open space. In practical applications, the free-flow velocities are usually assumed to be normally distributed about a measured mean [14]. Negative free-flow velocities and free-flow velocities above the sprint world record should be excluded. The influence of the reaction time $\tau$ modeled by prefactor $\frac{1}{\tau}$ is not relevant for our investigations at the moment and $\tau$ is set to 0.5 (seconds) as suggested in [5] throughout the paper. Again, in practical simulations, the reaction time should be individually set.

Stating a problem in dimensionless form often makes it easier to focus. In the case of a single pedestrian with just one target, this can be achieved by the transformations $\tilde{t} = \frac{1}{\tau}t$ for a dimensionless speed, $\tilde{x} = \frac{x}{\tau v_0}$ for a dimensionless pedestrian position leading to $\tilde{v} = \frac{v}{v_0}$ as dimensionless speed. For the equations we return to $x$ and $v$ as variables. The dimensionless system is

$$\dot{x} = v, \quad \dot{v} = \left(-\frac{x}{\|x\|} - v\right). \tag{5}$$

The simplified model versions in Eqs. (3) and (5) highlight that, while inspiration for the social force model stems from molecular dynamics, it is not, in itself, a Hamiltonian system. That is, there is no Hamiltonian function $H(x,v)$ to rewrite the system in the form

$$\dot{x} = \nabla_v H(x,v), \quad \dot{v} = -\nabla_x H(x,v) \tag{6}$$

and to represent energy. From (6) follows that the Hamiltonian must have the form

$$H(x,v) = \tfrac{1}{2}\langle v,v\rangle + G(x) \tag{7}$$

for some $G$. See [10] for a longer discussion. With this, the term $-\frac{1}{\tau}v$ in (4) can not be produced. In fact, term $-\frac{1}{\tau}v$ introduces "friction" and destroys energy conservation; so does the speed cutoff in Eq. (1). This means that the wealth of methods developed to conserve physical quantities that are characteristic for the Hamiltonian systems of molecular dynamics do not target the social force model. In fact, they very often explicitly use the separable form of the Hamilton function (7). Prominent examples are symplectic splitting methods that conserve the volume in phase space. They are described in [10] or [11].

So, instead of trying to reproduce physical conservation laws that do not apply for pedestrian motion, we turn our attention to a straightforward analysis of the mathematical properties of the system: unit vectors $-x/\|x\|$ point in the direction of the the target for all locations $x \neq (0,0)$. However, the function $F$ has a singularity at the target $x = (0,0)$. The right hand side displays a jump (see Fig. 1).

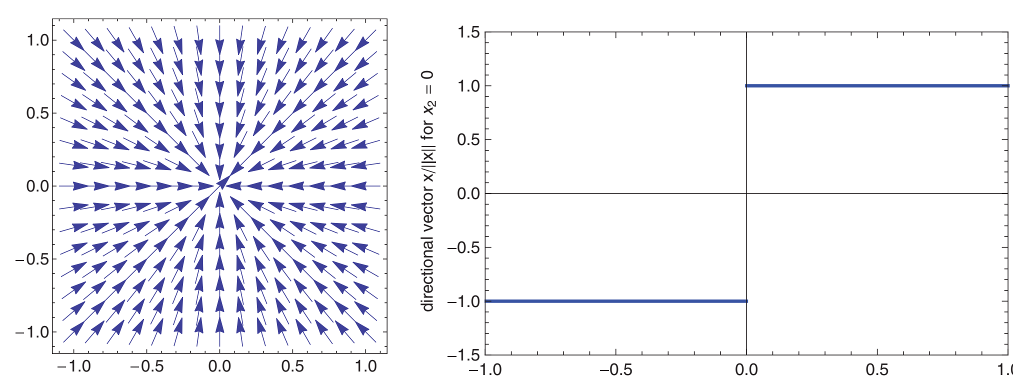


FIG. 1. (Color online) Discontinuity in the right hand side of the social force model at the target. Left: vector plot. Right: cut with the plane $x_2 = 0$.

Singularities in an equation do not necessarily shock the practical user nor do they keep a model from being useful. However, they do have consequences, some of them undesirable. In our case, the disadvantages are twofold:

*Loss of smoothness*. A jump in the derivative means that the solution, if it exists, is at best continuous, certainly not differentiable. Such a solution can only exist in a weak sense.

*Loss of accuracy and speed of convergence*. More important to the practical user is the loss of accuracy, in fact of convergence, of numerical schemes near discontinuities. This means that, whenever a virtual person in the social force model comes close to an intermediate target, or any other point with insufficient smoothness in $F$, the trajectories and the velocities will no longer be well resolved even with very small step sizes $\Delta t$. Oscillations and even collisions in the numerical approximation of the supposed true trajectories are the result. This happens even at a very short range. It also means that higher order, fast converging schemes, such as the Runge-Kutta methods, can not unfold their potential and one is stuck with slow converging schemes such as Euler's method. We demonstrate this in Sec. IV. In the worst case, numerical error or, more likely, the force of another pedestrian may cause a virtual person to stumble right on the target point, or very close to it. This would lead to numerical division by zero. In a practical simulation, one observes wild oscillations in the pedestrian trajectories or even that one virtual pedestrian is "blown away" from the target. In fact, it is not difficult to construct a "pathological" example using the Euler scheme for the numerical solution as we see in Sec. II B1.

One may argue that a virtual person can be removed from the simulation in time before he or she reaches the target. This means that the set of differential equations must be reinitialized with one less person. In fact, after reinitialization, we have a new and slightly different set of equations with a different solution. This constitutes a drawback, but may work from a practical perspective as long as one does not use intermediate targets to guide the virtual pedestrians along a desired path and around obstacles. However, intermediate targets are almost indispensable in practical applications. An early handover to the next target as soon as it is within sight, which is equivalent to another reinitialization and switch to a slightly altered initial value problem, helps. It is also natural from a modeling point of view: Pedestrians like to navigate along a graph where the points of orientation are connected by a direct line of sight [15]. However, this is still tricky to handle. A lot of manual calibration for each intermediate target may become necessary to get just the right handover moment: On the one hand, one strives to avoid the numerically difficult close vicinity of the target. On the other hand, the risk of losing sight of the new intermediate target increases with early handover. Another person might "push" the virtual pedestrian out of the direct line of sight and he or she becomes trapped. Thus, once several pedestrians are competing for space at the intermediate target exerting forces on each other, the calibration may become dysfunctional. We show a situation where this happens in Sec. V.

#### 1. *Explicit Euler scheme: Stable orbits around the target*

The solution of the difference equations that stems from discretizing a differential equation through a numerical scheme need not conserve the behavioral properties of the original equation. This happens to be the case when one applies Euler's explicit method on (3). Applying a $k$-step numerical scheme on a differential equation

$$\dot{y} = \mathcal{F}(y) \tag{8}$$

means to discretize the equation in time. In the case of Euler's method, the result simply is

$$y_n = y_{n-1} + \Delta t \mathcal{F}(y_{n-1}), \tag{9}$$

where $y_n$ is the solution one step ahead in time from $y_{n-1}$ and $\Delta t$ is the step size in time.

Even with a consistent numerical scheme, such as Euler's method, there is no guarantee that the solution of the difference equation has the same properties as the (supposed) solution of the differential equation, unless a number of restricting conditions on the smoothness of the right hand side are satisfied. In the case of the social force model with its discontinuity in the right hand side at the target point, and nondifferentiability at several other locations, we do not profit from such a comfortable situation.

Indeed, the explicit Euler scheme which is widely popular in the social force community, despite its poor speed of convergence, reveals very undesirable behavior. The trajectories of the corresponding difference equation show a stable orbit around the target. They do not, as required, approach the target when time goes to infinity. A particularly bad case is easily constructed with with $\tau = 0.5$, free-flow velocity $v_0 = 1$, step size $\Delta t = 0.5$, and initial values $x = (0.25,0)$ and $v = (1,0)$. The Euler scheme produces alternating values with $x_1 \in \{-0.75,-0.25,0.25,0.75\}$, $v_1 \in \{-1,1\}$ and $x_2 = 0$ and $v_2 = 0$ for all iterations. Since the pedestrians keep moving at full speed, that is 1 m/s, each step in time corresponds to a stride with fixed length 0.5 m. Obviously, the pedestrians will never get close to the target. Even worse, with $(x,v) = [(0.5,0),(-1,0)]$ as starting point, the second iteration lands exactly on the target $x = (0,0)$ leading to division by zero and abortion of the simulation run. The step sizes in these bad case examples are admittedly coarse but serve to demonstrate the principle, namely, that the numerical solution may never get close to the target but may oscillate around it at considerable speed or, even worse, that division by zero is quite possible.

Figures 2 and 3 show other orbits for step sizes $\Delta t = 0.5$ (seconds) and 0.1 (seconds). The latter would be a reasonable step size corresponding to a spatial resolution of roughly 10 cm for each time step, or about $\frac{1}{8}$ of a typical stride length [4], in a simulation with a realistic free-flow velocity of about 1 m/s. However, the orbits keep the pedestrians at a distance of about 67 and 13 cm, respectively, from the target, a lack of aiming accuracy that does not seem negligible. An orbit sufficiently close to the target would remedy this shortcoming, at least from a practical point of view. Unfortunately, this is only true for smaller step sizes in time, which increase the simulation time. Also, even with smaller step size $\Delta t$, the pedestrian keeps moving at a fast speed.

### C. Singularity of the repulsive forces when pedestrians collide

Following the suggestion in [5] for a suitable potential, the repulsive force between two pedestrians $i$ and $j$, as seen from

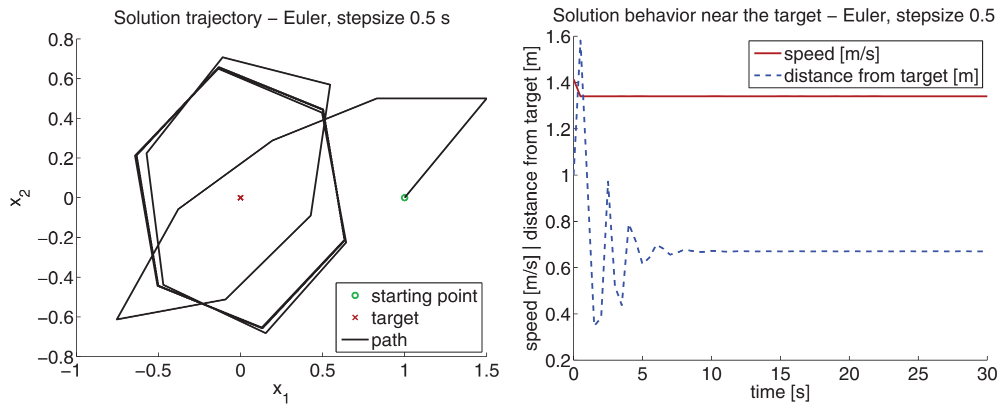


FIG. 2. (Color online) Euler's scheme to solve the SFM develops a stable orbit around the target, never reaching the target and never slowing down. With step size in time $\Delta t = 0.5$ s and free-flow velocity 1.34 m/s, the person remains about 0.67 m off target and keeps moving at full speed.

pedestrian $i$, is given by

$$F_{\mathrm{ped},i,j} = \frac{x_i - x_j}{\|x_i - x_j\|}\frac{V^0}{\sigma}e^{-\frac{\|x_i - x_j\|}{\sigma}}, \tag{10}$$

where $x_i$ denotes the position of pedestrian $i$.

For simplicity, we stick to a circular shape of the pedestrians. Parameters $V^0$ and $\sigma$ vary the strength and reach of the force. Calibration should ensure that pedestrians do not overlap in standard situations. Unfortunately, this is a delicate task that has yet to be completed to full satisfaction [8]. Calibration, however, is not the goal of this paper. So, we use the parameter choices $V^0 = 2.1\ \mathrm{m}^2/\mathrm{s}^2$ and $\sigma = 0.3$ m from [5] despite the fact that we observe overlapping in simple situations (see Sec. IV).

The force contains the term

$$\frac{x_i - x_j}{\|x_i - x_j\|} \tag{11}$$

that becomes singular whenever $x_i = x_j$. However, unlike before, there is no attraction pointing towards the singularity. Quite the contrary, the repulsive forces increase with decreasing distance between the torsos' midpoints. Thus, only total collision would have a numerical impact on a simulation run.

### D. Loss of differentiability at the desired speed

The speed cutoff in (2) means that the right hand side of (2) is not differentiable for all velocities $w$ with $\|w\| = v_{\max}$. Following we show an example of a numerical experiment with speed cutoffs. We let a pedestrian start from position $x = (1,0)$ with velocity $w = (1,1)$ while the target is at (0,0) (see Fig. 4). The maximum acceptable speed is set to $1.3 v_{i,0}$ with free-flow velocity $v_{i,0} = 1.34$ m/s as suggested in [5]. Using a fifth order Runge-Kutta scheme with a step size $\Delta t = 0.5$, we observe speed cutoffs when approaching the target. Note that this step size is not coarse for the fast converging Runge-Kutta method applied on the social force model as long as no singularities are encountered (see Sec. IV). We did not often observe speed cutoffs in our numerical experiments, but they can not be excluded. Hence, if one wishes to successfully use a high performing numerical scheme, one needs to deal with the situation.

### E. Loss of differentiability at obstacle corners

The obstacle potential perceived by each virtual pedestrian as suggested in [5] depends on the distance of the pedestrian from the obstacle. If the boundary of the obstacle is not smooth,

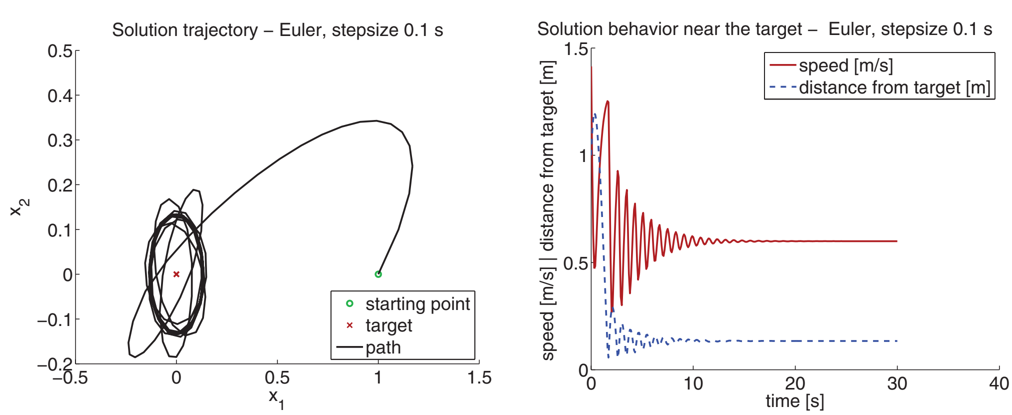


FIG. 3. (Color online) Euler's scheme to solve the SFM develops a stable orbit around the target, never reaching the target and never slowing down. With step size in time $\Delta t = 0.1$ s and free-flow velocity 1.34 m/s, the person remains about 0.13 m off target and keeps moving at about half speed.

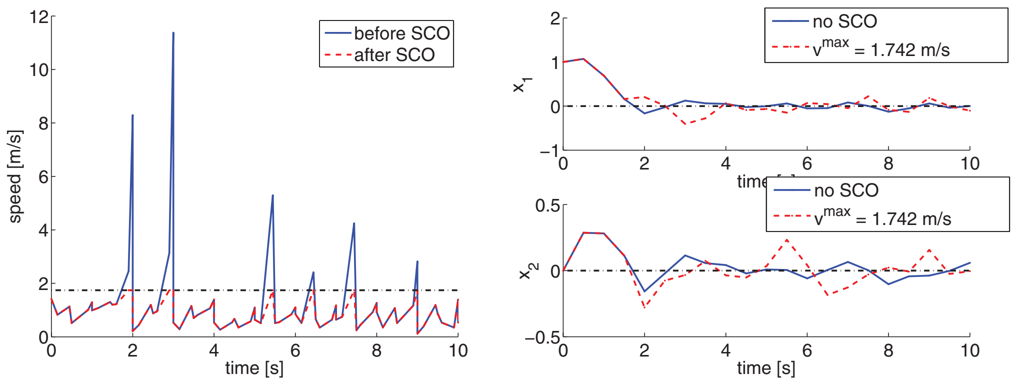


FIG. 4. (Color online) Left: Speed cutoffs observed for a single pedestrian approaching the target. Right: Influence on the position $(x_1,x_2)$. The solid (blue) curves show results entirely without speed cutoff. The dashed (red) curves are with speed cutoff. As soon as the speed reduction takes place for the first time the equations and hence the solutions no longer coincide.

the resulting distance function and hence the obstacle potential and right hand side of the differential equation (2) will not be smooth. Again, this leads to increased errors in the numerical solution and loss of convergence especially with higher order schemes.

## III. MOLLIFIED MODEL

In this section, we introduce mollifications of the classic social force model (2) for each area where the continuity or differentiability was lost. The resulting mollified social force model (MFSM) has a smooth right hand side and thus a solution for each time interval $[t^s,t^{\text{end}}]$ for each initial value $(x^s,v^s)$. The Jacobian matrix is bounded so that a solution exists for $t \to \infty$. The solution has an asymptotically stable steady state in $(x,v) = 0$, at least in the case when a single person approaches the target. Last but not least, the differentiability remedies the numerical problems.

There are also methods to detect discontinuities and restart the solution algorithm after the discontinuity that might be successfully employed (see [16]). In this work, we do not follow this approach because we think that the model itself becomes a better approximation to reality after mollification.

### A. Mollification at the target

We look at the simplified formulation of the social force model with a single pedestrian and only one target: Eq. (3) [or (5) in the the dimensionless form]. The arguments in this section are identical for both formulations. The cause for the stability and convergence issues close to the target is the loss of continuity at the target point. We replace the directional vector $-\frac{x}{\|x\|}$ by

$$-\frac{x}{\sqrt{x_1^2 + x_2^2 + \epsilon^2}} \tag{12}$$

in Eq. (4). Clearly, this mollified version of the model is continuous and infinitely often differentiable at the target. Thus, we know from the theory of initial value problems that there exists a unique solution for each initial value $u := (x^s,v^s)$. Also, the target point with zero speed is a steady state solution. The eigenvalues of the Jacobian matrix all have negative real parts $(-\frac{1}{2})$ so that we immediately get local asymptotic stability. Nonzero imaginary parts, which are the rule, produce spiraling orbits towards the target.

In other words, provided the starting value is sufficiently close to the steady state, the solution converges asymptotically to the steady state: the pedestrian moves towards the target

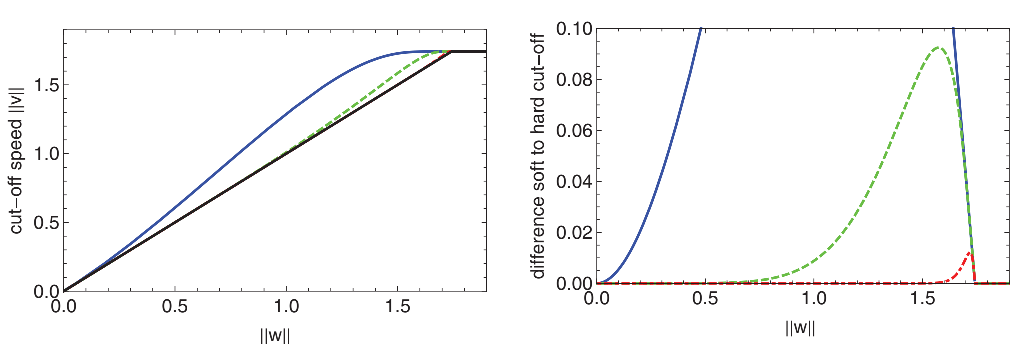


FIG. 5. (Color online) Mollification of speed cutoff: The figure on the left compares $\|v\|$ of the hard cutoff (solid black line) with mollifications for $p = 2$ (solid, blue), 8 (dashed, green), 64 (dotted-dashed, red). The last is hardly visible on top of the hard cutoff. The figure on the right displays the maximum difference between the speed $\|v\|$ of the original and the mollified versions for $p = 2$ (solid, blue), 8 (dashed, green), 64 (dotted-dashed, red). The value of $\tilde{\epsilon}^2$ was chosen sufficiently small that its effect is invisible in the plot.

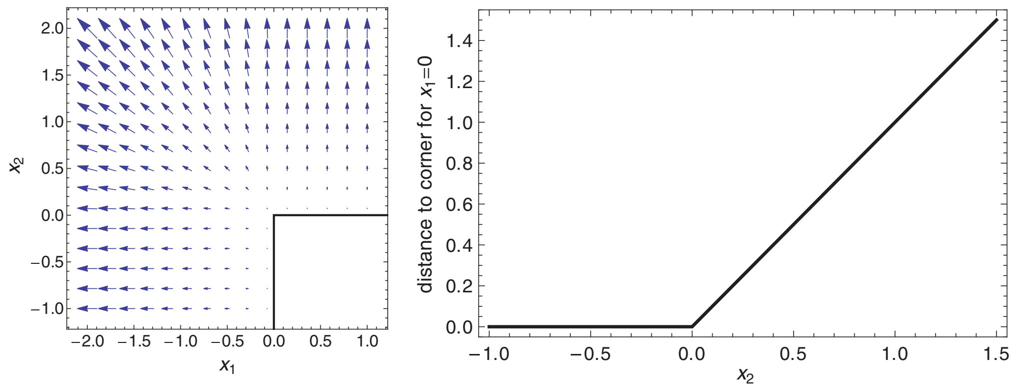


FIG. 6. (Color online) Left: Vector plot of distance to corner. The corner is in (0,0). In $(x_1,x_2)$ arrows indicate in which direction the distance is measured and, by the length of the arrow, how big the distance is. Right: The emerging fan is continuous but not differentiable as one sees when one plots the distance in dependency of $x_2$ for fixed $x_1 = 0$.

while steadily decreasing the speed. This behavior is desirable in itself, but it also leads to a much better numerical performance as we demonstrate in Sec. IV. The eigenvalues show that the mollified equation is not stiff so that the Euler scheme and the Runge-Kutta scheme used in Sec. IV are suitable numerical solvers.

We even get global asymptotic stability using Lyapunov's method and La Salle's stability theorem [11,17]. We get a weak Lyapunov function with

$$L(x,v) := \sqrt{x_1^2 + x_2^2 + \epsilon^2} + \tfrac{1}{2}\langle v,v\rangle - \epsilon \tag{13}$$

with $\|L(x,v)\| \to \infty$ for $\|(x,v)\| \to \infty$. Lasalle's theorem ensures global asymptotic stability. Hence, whatever initial position and initial velocity a person has, he or she will be drawn to the target point and never escape. Close to the target, the velocity becomes infinitesimally small.

Even with very small $\epsilon$ in the denominator of (12), the speed is reduced compared to the original speed in the social force model. In this paper, we chose $\epsilon^2 = 0.1$ to demonstrate the effect. This would introduce a speed reduction of about 5% at a velocity of about 1 m/s, which might be still a little high to neglect.

The arguments above can not be applied to the the original social force model because its right hand side is discontinuous. Particular solutions are known in special cases, but the authors are not aware of a general proof of existence for a weak solution of the social force model. A typical method to prove existence is to look for a limit function of the solution of the mollified model for $\epsilon \to 0$. If such a limit exists, it is a candidate for a weak solution of the original equations.

### B. Mollification for pedestrians competing for space

Unlike the singularity at the target, the singularities in the forces acting between pedestrians are unlikely to have an impact on the numerical performance. Still, to get rid of the singularity, one may introduce a mollifying term $\epsilon_{\text{interaction}}$ as in (12) replacing (11) by

$$\frac{x_i - x_j}{\sqrt{(x_{i,1} - x_{j,1})^2 - (x_{i,2} - x_{j,2})^2 + \epsilon_{\text{interaction}}^2}}. \tag{14}$$

Unfortunately, this has a severe drawback: The repulsive force between pedestrians is no longer strongest when the pedestrians completely overlap, but decreases when the pedestrians' centers become very close. In fact, with $\epsilon_{\text{interaction}}^2 = 0.1$,

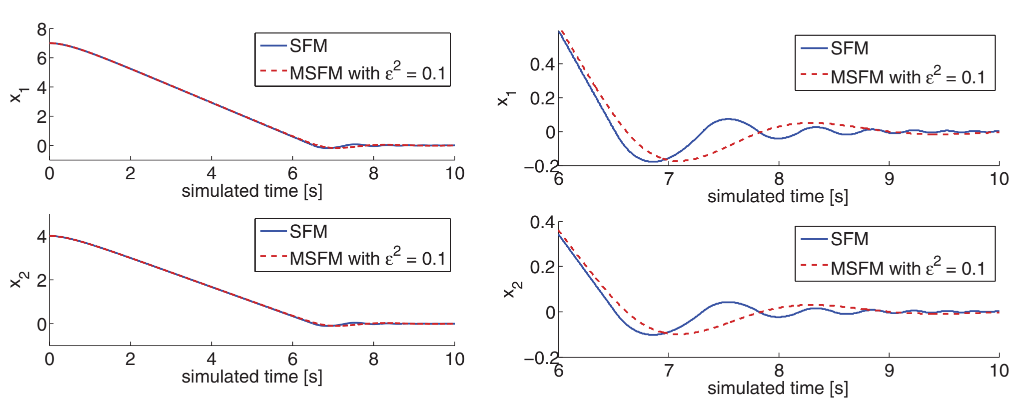


FIG. 7. (Color online) Component wise comparison of a pedestrian trajectories for the SFM and the MSFM. Scenario: A single person moves from position (7,4) to the target at (0,0) starting with a speed of 0 m/s. The desired velocity of the person is set to 1.34 m/s. Relaxation time $\tau = 0.5$ s. Mollification parameter $\epsilon^2 = 0.1$. Right: Focus on time $t > 6$ where the solution trajectory starts to go back and forth through the target.

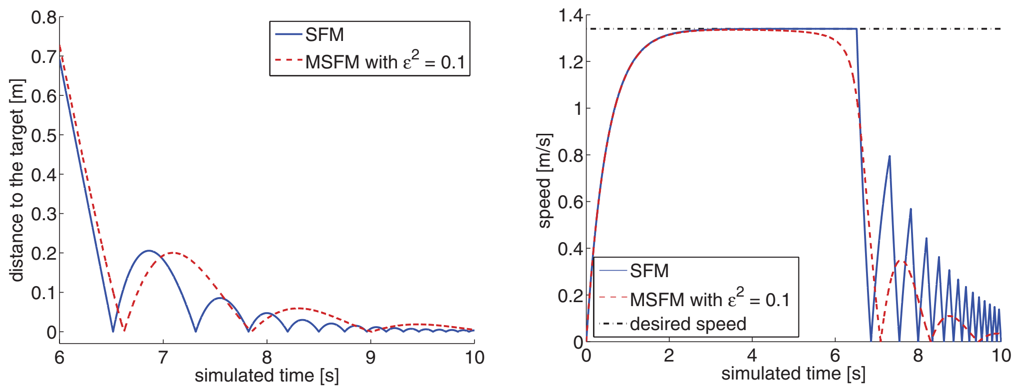


FIG. 8. (Color online) Comparison of the pedestrian's distance to the target and speed for the SFM and the MSFM. Scenario: A single person moves from position (7,4) to the target at (0,0) starting with a speed of 0 m/s. The desired velocity of the person is set to 1.34 m/s. Relaxation time $\tau = 0.5$ s. Mollification parameter $\epsilon^2 = 0.1$. Focus on time $t > 6$ where the solution trajectory starts to go back and forth through the target.

total collisions can be easily observed. To avoid this, and nonetheless ensure numerical peace of mind, we suggest to use extremely small values for $\epsilon^2_{\text{interaction}}$, some order of magnitude smaller than the numerical error one may reasonably aim for. When experimenting with the relatively big $\epsilon^2_{\text{interaction}} = 10^{-3}$, we neither observed numerical problems from collisions nor complete overlapping among the colliding pedestrians.

Another feasible way to deal with the problem is to set the repulsive force to zero if the centers of two pedestrians coincide, truly or numerically. This can be justified by multiplying the original repulsive force (11) by an infinitesimally smooth function that is equal to 1, except in a very small sphere around the repelling pedestrian's midpoint, and vanishes at the midpoint $x_j$. The result is a repulsive force that is almost identical to (11), but zero where the original force is infinite. Such a mollifying function can be constructed from the test function on compact support that we need in the next section [see Eq. (15)]. Knowing the exact function is unnecessary for the application of a numerical scheme.

### C. Mollification of the speed cutoff

The velocity $\dot{x} = v(w)$ in Eq. (2) is not differentiable because it is cut off at $\|w\| = v_{\max} > 0$. We suggest to replace the cutoff by an infinitely smooth ram-up function and thus to get rid of any numerical difficulties that the singularity in the social force model might cause. We get our inspiration from the theory of distributions: We slightly generalize the kernel of the Friedrichs' mollifier, an infinitely smooth function with compact support [18]. For $p \in \mathbb{N}$,

$$f_m(w,p) := \begin{cases} e e^{\left(-\frac{1}{1-(\frac{\|w\|}{v_{\max}})^{2p}}\right)} & \text{if} \quad \|w\| < v_{\max}, \\ 0 & \text{else.} \end{cases} \tag{15}$$

A mollified version of $v(w)$ is given by

$$v(w,p) := f_m(w,p)w + [1 - f_m(w,p)]v_{\max} \times \frac{w}{\sqrt{w_1^2 + w_2^2 + \tilde{\epsilon}^2}}. \tag{16}$$

Function $v$ is smooth and never exceeds $v_{\max}$, but slightly overestimates the velocity of (2). That is, deceleration is slightly delayed compared with the hard cutoff. The impact of this can be made negligible by choosing parameter $p$ large enough. The term $\tilde{\epsilon}^2$ is necessary to avoid numerical division by zero at or close to $w = (0,0)$ (see Fig. 5).

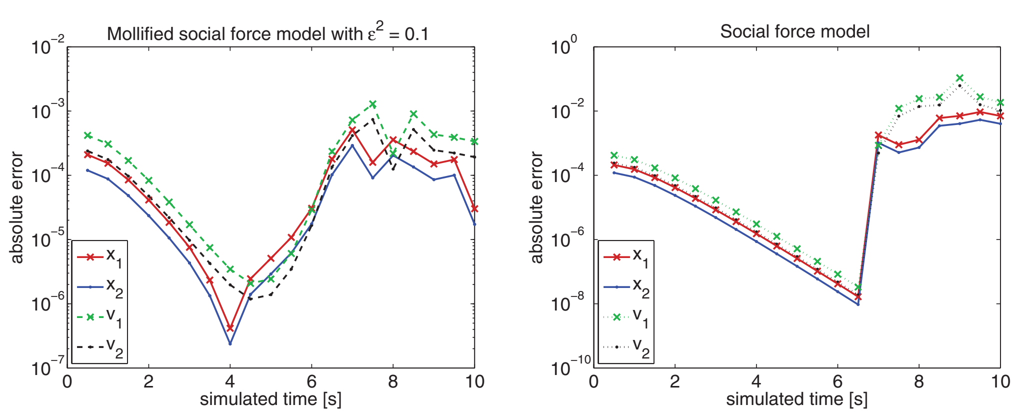


FIG. 9. (Color online) Error comparison for the mollified and classic social force model using Euler's method with step size $2^{-10} = 0.001$.

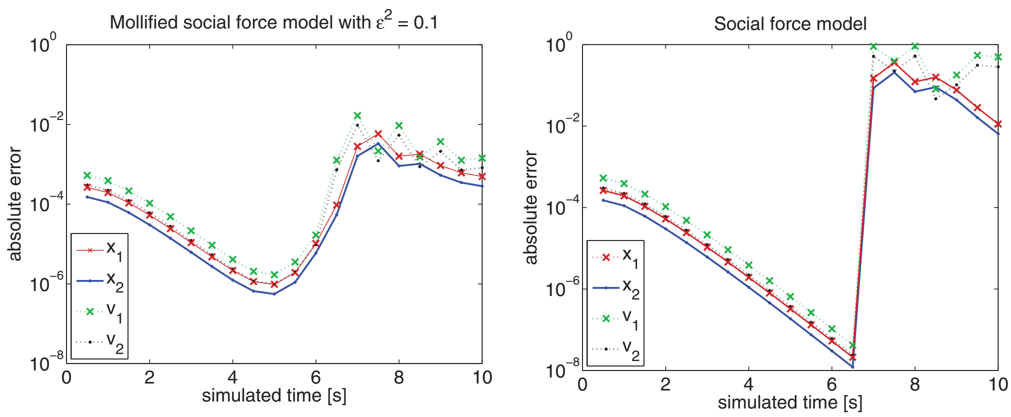


FIG. 10. (Color online) Error comparison for the mollified and classic social force model using a fifth order Runge-Kutta scheme with step size $2^{-1} = 0.5$.

### D. Mollification of the obstacle force

Realistic obstacles in a simulation scenario have corners that make the distance function from positions in the scenario a continuous but nondifferentiable function (see Fig. 6). There are three principal ways to mitigate this problem:

(i) *Mollification of the obstacle boundaries*. This is relatively easy to achieve using mollification techniques as in Sec. III C. However, smoothing corners will make the scenario unrealistic, if the smoothing is pronounced. Real objects have sharp corners. Nonetheless, for simplicity, we follow this approach when presenting an evacuation scenario in Sec. V.

(ii) *Mollification of the obstacle force function*. Mollification of the obstacle force function is a viable approach except at the corner points. A degradation of convergence in the close vicinity of corners will remain visible for coarser step sizes.

(iii) *Detection algorithms for discontinuities*. Discontinuities in the right hand side of an ordinary differential equation can be detected by a suitable numerical scheme and the solution scheme can be restarted after the discontinuity (see [16]). This might be an elegant way to avoid negative effects of sharp obstacle corners.

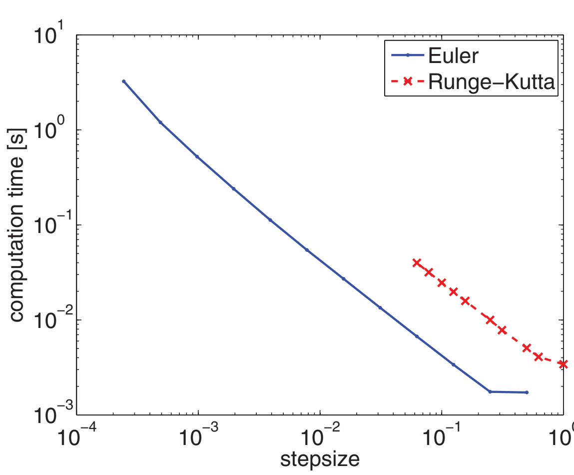


FIG. 11. (Color online) Computation time per step size. For a performance comparison, step sizes that produce comparable errors in the resolution of the trajectories and the velocity must be compared: e.g., $\Delta t = 2^{-1} = 0.5$ for the Runge-Kutta scheme compared to $\Delta t = 2^{-10} = 0.00098$ for Euler's method.

### E. Mollification for polygonial targets

It makes sense to use line targets or polygon targets, e.g., when approaching a door to make the virtual pedestrians use the full width of the bottleneck. Molnár defines an attractive force for a line target in his thesis [13]. The resulting force is continuous outside the target, but not differentiable. Hence, the same problems arise as for polygon obstacles in Sec. III D above. They can also be dealt with in the same way. In addition, it makes sense in many scenarios to replace the target polygon by objects with a smooth boundary, e.g., circles or ellipsoids.

## IV. ACCURACY AND CONVERGENCE OF NUMERICAL SCHEMES FOR THE CLASSIC AND MOLLIFIED SOCIAL FORCE MODEL

Numerical schemes to solve differential equations require, in order to work properly, a level of smoothness in the solution of the equation that matches the order of the scheme. For example, a first order scheme needs a twice differentiable solution. If this is not the case, accuracy is usually lost. The right hand side of the social force equation is the first derivative of the solution. It is not differentiable in several places and discontinuous at the target. Hence, the solution of the social force equations can not be smooth. It is at best continuous and any solution is a solution in the weak sense only. We must expect severe loss of accuracy in any of the nonsmooth locations. This is best demonstrated by computing the order of convergence of the numerical schemes when approaching critical locations. We select the popular, if slow converging, explicit Euler scheme and the highly efficient fifth order Runge-Kutta scheme that is the fifth order part of the default solver ode45 in Matlab, the Dormand-Prince scheme [19].

### A. Comparison of trajectories near the target

In the following scenario, a single person moves towards a target where force $F$ has its singularity in the original social

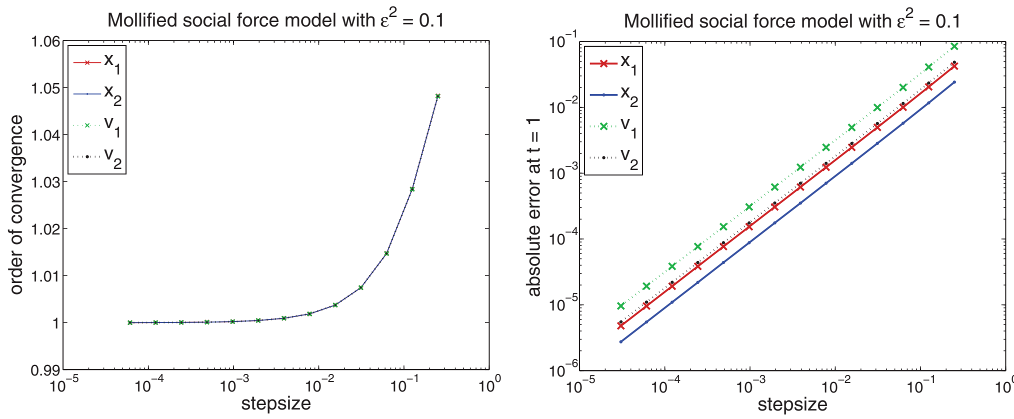


FIG. 12. (Color online) Order of convergence and absolute error for the mollified SFM with $\epsilon^2 = 0.1$ using Euler's method. Left: order of convergence (read from right to left). Right: absolute error.

force model. The initial velocity is set to $v_{\text{start}} = (0,0)$ so that the problem can be reduced to a one-dimensional problem, independently of the starting point, by rotating the coordinate system. We look at the absolute values of the solution components $(x_1,x_2)$ and $(w_1,w_2)$ and observe, as expected, that the oscillations in the mollified model version are significantly attenuated (see Figs. 7 and 8). Since oscillations do not match human behavior, this outcome seems highly desirable independently of numerical effects.

### B. Accuracy and numerical convergence comparison near the target

#### *1. Comparison of the absolute error when approaching the target*

We look at the global truncation error of the numerical solution at time $t$. It is given by the difference between the numerical solution $y_{\Delta t}(t)$ and the exact solution $y(t)$. One can either look at the Euclidean norm of the error or at the absolute values of the components of $e_{\text{tr}}$:

$$e_{\text{tr}}(t) = y(t) - y_{\Delta t}(t). \tag{17}$$

In our case, we have not computed the exact solution. Instead, a numerical solution with very small step size $\Delta t_{\text{small}}$ is used. Note that this only works if one can expect a significantly improved approximation when decreasing the step size. In the case of the original social force model, this means that one has to stay clear of the target.

We use the step sizes $\Delta t = 2^{-1} = 0.5$ for the fifth order Runge-Kutta scheme and $\Delta t = 2^{-5} = 0.03125$ for the Euler scheme to get approximately the same absolute error for both methods at a safe distance from the target. To compute the errors, each numerical solution is compared to a much finer approximation computed with the same scheme and $\Delta t = 2^{-15} = 3.05 \times 10^{-5}$. Then, we increase the simulated time $t$ thus approaching the target until $t_{\text{end}} = 10$ (s). Computing the numerical solution at $t_{\text{end}} = 10$ took 1.16 s with Euler's method, but only 0.01 s with the fifth order Runge-Kutta scheme, that is, the Runge-Kutta method was *116 times faster*. The advantage becomes even more pronounced with longer time periods and more pedestrians or, when step size control is used to restrict the use of small step sizes to the areas with fast changes in the solution.

In Figs. 9 and 10, we compare the absolute error of the social force model to its mollified version with $\epsilon^2 = 0.1$ as the pedestrian is getting closer to the target. For the original social force model, there is a pronounced jump in the error at about $t = 6.5$ when the solution trajectory $(x_1,x_2)$ starts to circle around the target. Both methods experience a dramatic loss

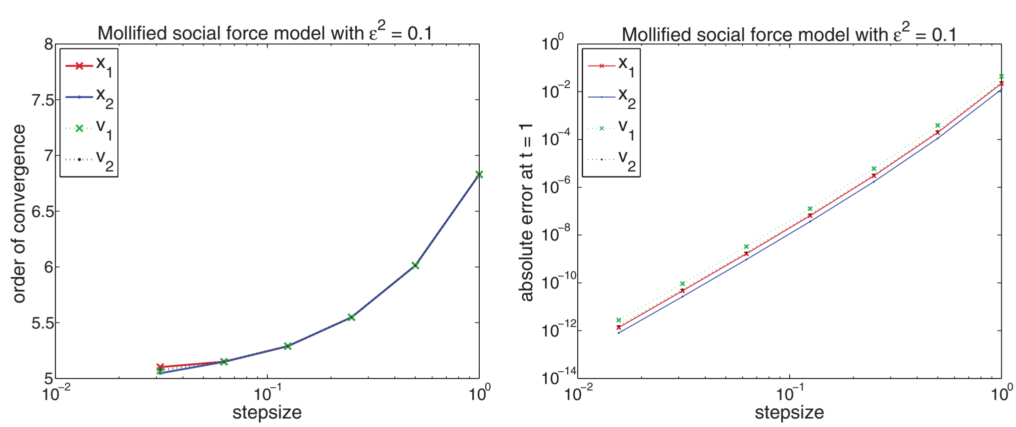


FIG. 13. (Color online) Order of convergence and absolute error for the mollified SFM with $\epsilon^2 = 0.1$ using the Runge-Kutta scheme. Left: order of convergence (read from right to left). Right: absolute error.

TABLE I. Absolute error and order of convergence for the mollified social force model with $\epsilon^2 = 0.1$ using Euler's first order method. The order of convergence for $x_1$ and $x_2$ as well as $v_1$ and $v_2$ coincide up to the accuracy considered here.

| | Absolute error | | | | Order of convergence | |
|---|---|---|---|---|---|---|
| $\Delta t_1$ | $x_1$ | $x_2$ | $v_1$ | $v_2$ | $x_1,x_2$ | $v_1,v_2$ |
| $2^{-2}$ | 0.0423165 | 0.0241808 | 0.0847043 | 0.0484025 | 1.04824 | 1.04818 |
| $2^{-3}$ | 0.0204625 | 0.0116928 | 0.0409612 | 0.0234064 | 1.02842 | 1.02838 |
| $2^{-4}$ | 0.0100317 | 0.00573237 | 0.0200816 | 0.0114752 | 1.01474 | 1.01472 |
| $2^{-5}$ | 0.00496486 | 0.00283706 | 0.0099389 | 0.00567937 | 1.00746 | 1.00745 |
| $2^{-6}$ | 0.00246963 | 0.00141122 | 0.00494386 | 0.00282507 | 1.00375 | 1.00374 |
| $2^{-7}$ | 0.00123161 | 0.000703778 | 0.00246553 | 0.00140887 | 1.00188 | 1.00188 |
| $2^{-8}$ | 0.000615005 | 0.000351432 | 0.00123116 | 0.000703522 | 1.00094 | 1.00094 |
| $2^{-9}$ | 0.000307302 | 0.000175601 | 0.000615181 | 0.000351532 | 1.00047 | 1.00047 |
| $2^{-10}$ | 0.000153601 | $8.77721 \times 10^{-5}$ | 0.000307491 | 0.000175709 | 1.00024 | 1.00023 |

of accuracy, but the loss is much worse for the Runge-Kutta scheme which does not tolerate the loss of differentiability. This clearly illustrates that singularities at intermediate targets are prone to ruin the resolution of pedestrian trajectories and make the use of high performing schemes pointless.

For the mollified model, on the other hand, no jump occurs. The error still increases for both numerical solutions, as must be expected when the true trajectories turn around narrow corners, but this time the error stays comparable. This means that, once again, the Runge-Kutta scheme can operate with a much larger step size to achieve the same resolution as the Euler scheme.

We also computed the $L_1$ and $L_2$ norms of the absolute error and obtained the same convergence behavior.

#### *2. Comparison of the order of convergence and computational speed*

We compute the order of convergence of Euler's method and the Runge-Kutta method for a scenario with a single pedestrian who stays at a safe distance to the target. As before, the exact solution is not known. Instead, we take numerical solutions computed for each scheme with step size $\Delta t = 2^{-15}$. We look at the absolute value of each error component.

A single pedestrian moves from position (0,1) towards the target at (0,0) starting with a speed of 0 m/s. The pedestrian's free-flow velocity $v_0$ is set to 1.34 m/s and the relaxation time $\tau$ to 0.5 s. At this distance to the target, the results with the social force model (SFM) and the mollified version (MSFM) are almost identical. Therefore, Figs. 11, 12, and 13 and Tables I and II only show the behavior of the mollified SFM.

#### *3. Computational speed*

Euler's method only needs one function evaluation per step as opposed to six for the Runge-Kutta scheme. In a naive comparison, where one only looks at the step size $\Delta t$ Euler's method would always appear advantageous in Fig. 11. However, to get a fair comparison, one must look at the error and compare the computation time for approximations with the same accuracy. Also, the scheme should operate with a step size where the order of convergence can be clearly observed so that the error estimate derived by comparing numerical solutions with different step sizes is reliable. The results in the last section suggested that for our scenario step sizes $\Delta t = 2^{-1} = 0.5$ for the Runge-Kutta method and $\Delta t = 2^{-10} = 0.00098$ for Euler's method must be compared to achieve an error of about $10^{-4}$ at a safe distance from the target and of about $10^{-2}$, corresponding to 1 cm in spatial resolution, close to the target. Then, Fig. 11 clearly favors the Runge-Kutta scheme.

Now, we use various step sizes and compare Euler's method and the Runge-Kutta scheme. At a safe distance to the target, the order of convergence fully develops. When one neglects round-off errors that are introduced through the limited machine precision, the order of convergence of a numerical scheme is given by

$$p = \lim_{\Delta t_1 \to 0} \frac{\ln\left(\frac{\|e_{\text{tr}}(\bar{y},\Delta t_2)\|}{\|e_{\text{tr}}(\bar{y},\Delta t_1)\|}\right)}{\ln\left(\frac{\Delta t_2}{\Delta t_1}\right)} \quad \text{with} \quad \Delta t_2 = \frac{1}{2}\Delta t_1, \tag{18}$$

TABLE II. Absolute error and order of convergence for the mollified social force model with $\epsilon^2 = 0.1$ using the fifth order Runge-Kutta method.

| | Absolute error | | | | Order of convergence | | | |
|---|---|---|---|---|---|---|---|---|
| $\Delta t_1$ | $x_1$ | $x_2$ | $v_1$ | $v_2$ | $x_1$ | $x_2$ | $v_1$ | $v_2$ |
| $2^{0}$ | 0.0220833 | 0.012619 | 0.0441317 | 0.0252181 | 6.8289 | 6.8289 | 6.82898 | 6.82898 |
| $2^{-1}$ | 0.000194249 | 0.000111 | 0.00038817 | 0.000221812 | 6.01275 | 6.01275 | 6.01236 | 6.01236 |
| $2^{-2}$ | $3.00843 \times 10^{-6}$ | $1.7191 \times 10^{-6}$ | $6.01343 \times 10^{-6}$ | $3.43625 \times 10^{-6}$ | 5.54832 | 5.54832 | 5.54805 | 5.54805 |
| $2^{-3}$ | $6.42878 \times 10^{-8}$ | $3.67359 \times 10^{-8}$ | $1.28527 \times 10^{-7}$ | $7.34438 \times 10^{-8}$ | 5.28923 | 5.28918 | 5.28905 | 5.28906 |
| $2^{-4}$ | $1.64404 \times 10^{-9}$ | $9.39481 \times 10^{-10}$ | $3.28723 \times 10^{-9}$ | $1.87841 \times 10^{-9}$ | 5.14993 | 5.14845 | 5.14895 | 5.14921 |
| $2^{-5}$ | $4.63052 \times 10^{-11}$ | $2.64881 \times 10^{-11}$ | $9.2649 \times 10^{-11}$ | $5.29325 \times 10^{-11}$ | 5.10201 | 5.04635 | 5.06938 | 5.0777 |

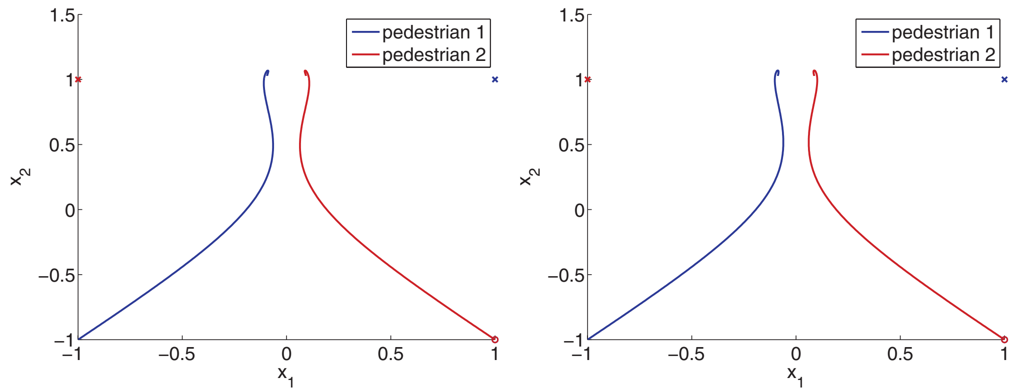


FIG. 14. (Color online) Trajectories for two pedestrians whose paths cross. The pedestrians are trapped in a deadlock. Left: $\epsilon^2_{\text{interaction}} = 0$. Right: $\epsilon^2_{\text{interaction}} = 0.001$.

where $e_{\text{tr}}(\bar{y},\Delta t)$ is the error for the numerical approximation $\bar{y}$ with step size $\Delta t$ and $\|\ldots\|$ is a suitable norm. We evaluate formula (18) for a sequence of step size pairs, halving step size in each iteration. For a convergent scheme, the order $p$ should emerge clearly with decreasing step sizes until the error approaches machine precision.

Figure 12 and Table I show the order of convergence and absolute error for Euler's method. The first order convergence is immediately visible and improves further with decreasing $\Delta t$. Figure 13 and Table II show the order of convergence and absolute error for the Runge-Kutta method. Convergence of $p$ to 5, the order of the Runge-Kutta scheme, is evident. With $\Delta t = 2^{-1}$ the error is already extremely small.

### C. Performance comparison with and without mollification of pedestrian repulsion

The high repulsion at the moment where two pedestrians would overlap completely makes this event highly improbable in the exact solution. Hence, a complete overlap, and division by zero, could only be caused by numerical error and hence faulty resolution of the pedestrian trajectories. This small danger can be removed by adding a mollification parameter to the repulsion force denominator as described in Eq. (14). Otherwise, the results do not change. We illustrate this with a scenario where two identical pedestrians cross paths. The two pedestrians start from $(-1,-1)$ and $(1,-1)$, respectively, towards their targets at $(1,1)$ and $(-1,1)$. The starting velocity for both is 0, the free-flow velocities are identical at 1.34 m/s. We use $\epsilon^2_{\text{interaction}} = 0.001$ because with a greater value the pedestrians would pass through each others' centers. With sufficiently small $\epsilon_{\text{interaction}}$, there is no significant difference between the classic social force model and the version with mollified pedestrian repulsion.

However, the pedestrians are trapped in a deadlock. Also, the pedestrians' centers are only 13 cm apart at the closest point. That is, they overlap for the parameter choices given in [5]. In fact, we observe that without careful calibration, partial collisions where real bodies would overlap are quite common. The problem becomes much more severe with poor resolution of the trajectories near nonmollified targets and obstacles (see Figs. 14 and 15).

## V. PERFORMANCE COMPARISON OF THE CLASSIC AND THE MOLLIFIED SOCIAL FORCE MODEL AT A BOTTLENECK

In this section, we compare the performance of numerical schemes that produced similar errors in the solution for the test

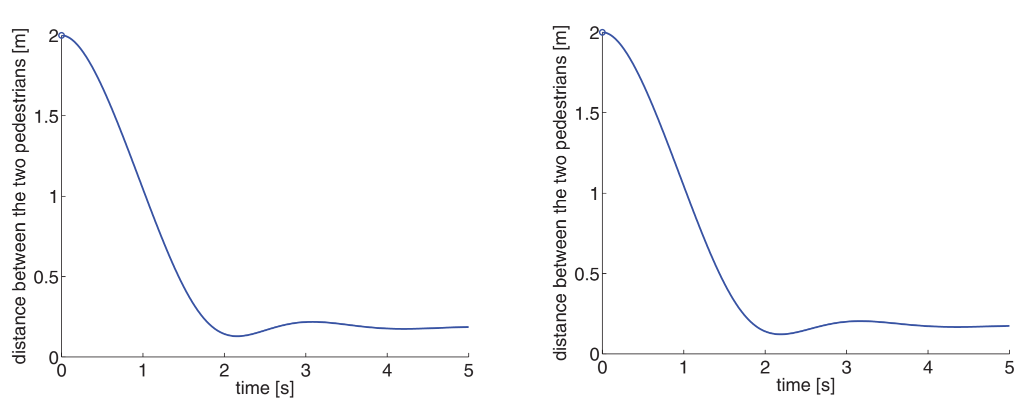


FIG. 15. (Color online) Distance between the two pedestrians trajectories. The pedestrians are trapped in a deadlock. Left: $\epsilon^2_{\text{interaction}} = 0$. Right: $\epsilon^2_{\text{interaction}} = 0.001$.

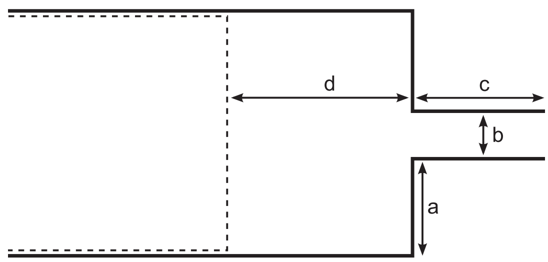


FIG. 16. Benchmark scenario from [12]. An intermediate target is placed in the middle of the door. The final target is at a safe distance to the right outside the corridor.

examples in Sec. IV. We look at a typical benchmark example inspired by [12]. $N$ virtual persons are placed in a room of length 20 m and width 7 m. At one end of the room is a centrally placed door of width 1 m that leads to a corridor of the same width. An intermediate target is placed in the middle of the door. The final target is at a safe distance to the right outside the corridor (see Fig. 16).

Handover from the intermediate target to the final target takes place when a person is no more than 0.4 m away from the door and the final target is in the direct line of sight (neglecting other pedestrians that may block the view). All pedestrians are identical, that is, they have the same free-flow velocity. This is unrealistic and leads to extremely symmetric trajectories. Variation of the free-flow velocities would immediately destroy the symmetry and yield more realistic trajectories. However, the symmetry is deliberate because it helps to demonstrate the effects of insufficient resolution.

Again, we use the explicit Euler scheme for the SFM and the fifth order Runge-Kutta scheme for the mollified SFM. In both cases, we set $\Delta t = 0.1$ so that an acceptable resolution may be expected for Euler's method as long as we stay away from locations with discontinuities of the right hand side or its derivatives: compare Tables I and II. In the scenario with one person and one target, the error for Euler's method was

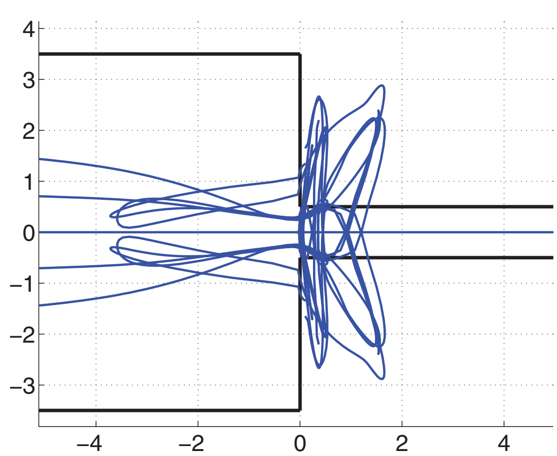


FIG. 17. (Color online) Virtual pedestrians move from left to right through a bottleneck. Numerical solution of the social force equations with Euler's method and step size $\Delta t = 0.1$.

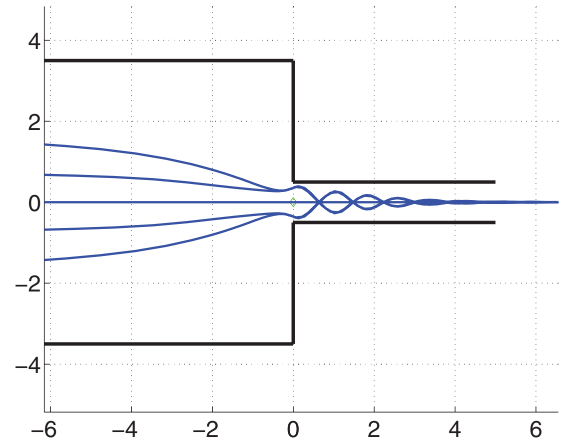


FIG. 18. (Color online) Virtual pedestrians move from left to right through a bottleneck. Numerical solution of the mollified social force equations with the fifth order Runge-Kutta method and step size $\Delta t = 0.1$.

below 0.01 m. When the pedestrian gets close to the target, Euler's method fails for the classic SFM. The Runge-Kutta scheme applied on the classic SFM would fare no better. However, when the discontinuity at the target is removed, the Runge-Kutta scheme encounters no more difficulties (compare Figs. 17 and 18).

## VI. CONCLUSIONS AND FUTURE WORK

In this paper, we showed how to remove discontinuities from the social force model's right hand side and its derivatives and thus defined a mollified model, the MSFM. We demonstrated that the solution of the mollified model is almost identical to the solution of the classic model, when the pedestrians are at a safe distance from the discontinuities. Hence, the desired dynamic properties of the social force model are conserved.

But, the new mollified model allows the use of high order fast converging numerical solvers, such as the Dormand-Prince scheme, increasing the computational speed, even in a very simple example, by a factor of 100. In view of future applications of pedestrian stream simulations that demand real time computation, e.g., training tools or prediction of immediate danger, the increase in numerical speed alone is very useful. In addition, the solution of the mollified model proved to be much more stable near the former problem zones, notably near intermediate targets. We observed less oscillations, less collisions, and no complete failures even for relatively coarse step sizes.

## ACKNOWLEDGMENTS

This work was funded by the German Federal Ministry of Education and Research through the project MEPKA on mathematical characteristics of pedestrian stream models (17PNT028). We would also like to thank F. Dietrich for valuable comments.

[1] S. Gwynne, E. Galea, M. Owen, P. Lawrence, and L. Filippidis, Build. Environ. **34**, 741 (1999).
[2] X. Zheng, T. Zhong, and M. Liu, Build. Environ. **44**, 437 (2009).
[3] A. Smith, C. James, R. Jones, P. Langston, E. Lester, and J. Drury, Safety Sci. **47**, 395 (2009).
[4] M. J. Seitz and G. Köster, Phys. Rev. E **86**, 046108 (2012).
[5] D. Helbing and P. Molnár, Phys. Rev. E **51**, 4282 (1995).
[6] D. Helbing, I. Farkas, and T. Vicsek, Nature (London) **407**, 487 (2000).
[7] M. Chraibi, A. Seyfried, and A. Schadschneider, Phys. Rev. E **82**, 046111 (2010).
[8] M. Chraibi, U. Kemloh, A. Schadschneider, and A. Seyfried, Networks Heterogeneous Media **6**, 425 (2011).
[9] B. A. Schlake, Diplomarbeit thesis, Institut für Numerische und Angewandte Mathematik, Universität Münster, 2008.
[10] M. Griebel, S. Knapek, G. Zumbusch, and A. Caglar, *Numerische Simulation in der Moleküldynamik* (Springer, Berlin, 2004).
[11] A. M. Stuart and A. R. Humphries, in *Dynamical Systems and Numerical Analysis*, edited by P. Ciarlet, A. Iserles, R. Kohn, and M. H. Wright (Cambridge University Press, Cambridge, UK, 1996).
[12] J. Liddle, A. Seyfried, and S. Boltes, in *Pedestrian and Evacuation Dynamics*, edited by R. D. Peacock, E. D. Kuligowski, and J. D. Averill (Springer, Berlin, 2011), pp. 833–836.
[13] P. Molnár, Ph.D. thesis, Universität Stuttgart, 1996.
[14] U. Weidmann, *Transporttechnik der Fussgänger*, 2nd ed., Schriftenreihe des IVT, Vol. 90 (Institut für Verkehrsplanung, Zürich, 1992).
[15] A. Kneidl, Ph.D. thesis, Methoden zur Abbildung menschlichen Navigationsverhaltens bei der Modellierung von Fußgängerströmen, 2013.
[16] E. Eich-Soellner, Ph.D. thesis, Universität Augsburg, 1991.
[17] J. L. Salle and S. Lefschetz, in *Stability by Liapunov's Direct Method-With Applications*, edited by R. Bellmann (Academic, New York, 1961).
[18] L. C. Evans, in *Partial Differential Equations* (American Mathematical Society, Providence, RI, 1997), p. 664.
[19] J. Dormand and P. Prince, J. Comput. Appl. Math. **6**, 19 (1980).